



# Formation, structure and climatic significance of blue rings and frost rings in high elevation bristlecone pine (*Pinus longaeva* D.K. Bailey)

J.C. Tardif <sup>a,\*</sup>, M.W. Salzer <sup>b</sup>, F. Conciatori <sup>a</sup>, A.G. Bunn <sup>c</sup>, M.K. Hughes <sup>b</sup>

<sup>a</sup> Centre for Forest Interdisciplinary Research (C-FIR), University of Winnipeg, 515 Portage Avenue, Winnipeg, MB, R3B 2E9, Canada

<sup>b</sup> Laboratory of Tree-Ring Research, The University of Arizona, 1215 E. Lowell St., Tucson, AZ, 85721, USA

<sup>c</sup> Department of Environmental Sciences, Western Washington University, Bellingham, WA, USA



## ARTICLE INFO

### Article history:

Received 12 May 2020

Received in revised form

21 July 2020

Accepted 22 July 2020

Available online 6 August 2020

### Keywords:

North America

High elevation

Tree rings

Latewood tracheid

Paleoclimatology

Climate extremes

536 and 1965 CE

Dust veil

Volcanic eruption

Holocene

## ABSTRACT

The study of anatomical irregularities in tree rings has recently gained momentum as a complement to traditional tree-ring measurements as they may provide information on extreme climatic events. Two anomalies, blue rings (BR) and frost rings (FR), were analyzed in bristlecone pine (*Pinus longaeva* D.K. Bailey) trees located along an elevation gradient in northeastern Nevada. These two subannual ring anomalies were systematically compiled for two periods; one centered on 536 CE (well-known for a volcanically-induced period of climatic cooling) and the other on 1965 CE (useful due to the availability of instrumental climate data). During the period 523–545 CE ( $n \geq 10$  trees), both BR and latewood FR (LWFR) were recorded abundantly in 532 and 536, as well as a BR cluster from 539 to 542 CE. Years when trees solely recorded a BR (without an accompanying LWFR) were more frequent in the earlier period than in the modern period (1954–2006 CE;  $n \geq 10$  trees) when both anomalies tended to co-occur. These results suggest a shorter growing season in the 536 period than in the 20th century. Modern BR/LWFR were most abundant in 1965 and 1978 CE. Both anomalies were mainly observed in the highest elevation trees and both were produced in years characterized by cooler than average temperatures throughout the growing season. Anatomically, BR and LWFR did not differ significantly in tracheid dimensions except that LWFR clearly showed damages associated with sub-freezing temperatures. The main feature distinguishing BR and LWFR from “normal” tree rings was a significant reduction in latewood secondary wall thickness. In *P. longaeva*, BR like pale latewood (light) rings, result from short and cool growing seasons which leads to reduced (or interrupted) lignification of tracheids. In species producing extremely narrow latewood like *P. longaeva* it may be difficult to macroscopically identify pale latewood years, thus rendering microscopic investigation of BR as a climate proxy useful in paleoclimatic research.

© 2020 Elsevier Ltd. All rights reserved.

## 1. Introduction

### 1.1. Tree-ring anomalies and climate

The study of tree-ring anomalies (anatomical irregularities), of their anatomical characteristics and of the environmental factors at their origin, in particular extreme climatic events, has recently regained attention in dendrochronology and paleoclimatology (Wimmer, 2002; Schweingruber, 2007; Bräuning et al., 2016). Such studies provide information on past environmental processes that occurred during the growing season of sets of trees (Tardif et al.,

2011; Hadad et al., 2020 and references below). Comparisons can then be made along environmental gradients and across temporal scales to help inform questions regarding ecological and climatic processes. Tree-ring anomalies can also provide an exactly dated proxy record of climate events occurring at local, hemispheric and global scales. Anomalies, like frost rings (Glerum and Farrar, 1966; LaMarche, 1970; Hantemirov et al., 2004; Gurskaya and Shiyatov, 2006; Waito et al., 2013; Gurskaya, 2014; Montwé et al., 2018; Hadad et al., 2019; Hadad et al., 2020; Barbosa et al., 2019), false rings (Wimmer et al., 2000; Hoffer and Tardif, 2009; De Micco et al., 2016) and pale latewood rings (also referred to as light rings; Brunstein, 1995; Szeicz, 1996; Gindl and Grabner, 2000; Girardin et al., 2009; Tardif et al., 2011; Montwé et al., 2018) have long been studied from a wood anatomical perspective and for their climatic significance. More recently the study of white earlywood

\* Corresponding author. Centre for Forest Interdisciplinary Research (C-FIR), University of Winnipeg, 515 Portage Avenue Winnipeg, Manitoba, R3B 2E9, Canada.  
E-mail address: [j.tardif@uwinnipeg.ca](mailto:j.tardif@uwinnipeg.ca) (J.C. Tardif).

rings (Waito et al., 2013), dark rings (Novak et al., 2016) and blue rings (Piermattei et al., 2015) have broadened understanding of environmental forcing on tree-ring formation.

Frost damage to xylem tissue during the active growing season has been linked to the production of frost rings (hereafter FR). These rings are characterized by the presence of collapsed/crushed/abnormal tracheids with lateral expansion and displacement of the rays (Glerum and Farrar, 1966; Schweingruber, 2007). The position of a FR within a tree's annual ring can also provide information regarding the timing of frost events (LaMarche and Hirschboeck, 1984; Gurskaya, 2014; Barbosa et al., 2019). Frost-ring intensity varies according to the level of cambial activity at the time of the event and also with the temperature and duration of the frost. Latewood FR (LWFR) have been observed in high-elevation Great Basin bristlecone pine (*Pinus longaeva* D.K. Bailey) and in Rocky Mountain bristlecone pine (*Pinus aristata* Engelm.). These cold-damaged rings have been associated with volcanically-forced cooling events (LaMarche and Hirschboeck, 1984; Brunstein, 1996; Salzer and Hughes, 2007). In contrast to LWFR, EWFR in bristlecone pine were reported to be scarce (LaMarche, 1970; LaMarche and Hirschboeck, 1984; Brunstein, 1995).

Blue rings (hereafter BR) were first identified in European black pine (*Pinus nigra* Arnold) and were defined as tree rings showing the presence of "... a continuous layer of unlignified axial tracheids occurring either in the earlywood or in the latewood" (Piermattei et al., 2015). Blue rings were observed after double staining tree-ring thin transverse sections (15–20  $\mu\text{m}$ ) with Safranin and Astra blue dyes. Cell walls that did not sufficiently lignify during the growing season take on the blue color (Piermattei et al., 2015). Blue rings were also recently described in Scots pine (*Pinus sylvestris* L.) trees growing in Romania (Semeniuc et al., 2016) and Latvia (Matisons et al., 2019), in lodgepole pine (*Pinus contorta* Dougl.) trees growing in western Canada (Montwé et al., 2018) and in *P. longaeva* trees growing in western United States (Hughes et al., 2016), again featuring the presence of under-lignified tracheids. The main hypothesis related to latewood BR formation calls for the observed lack of lignification in tracheids to be caused by low air temperature at the end of the growing season (Piermattei et al., 2015; Semeniuc et al., 2016). Similar climatic events are also believed to form pale latewood (light) rings (Szeicz, 1996; Gindl and Grabner, 2000; Gindl et al., 2000; Girardin et al., 2009; Tardif et al., 2011). In timberline spruce (*Picea abies* (L.) Karst.) light rings (LR) were shown to have latewood cells with reduced lignin content due to interference by cooler temperature towards the end of the growing season (Gindl and Grabner, 2000; Gindl et al., 2000). A delayed growing season as well as cooler early and late growing seasons have also been stressed (Szeicz, 1996; Girardin et al., 2009; Tardif et al., 2011). Interestingly, Brunstein (1995) mentioned that LR and LWFR often co-occurred in *P. aristata* trees. Hantemirov et al. (2004) also observed the co-occurrence of LR and FR in Siberian juniper (*Juniperus sibirica* Burgsd.) and in Siberian larch (*Larix sibirica* Ledeb.). Bräuning et al. (2016) suggested that the term BR may simply be another representation of LR using an alternative detection method. Montwé et al. (2018) implied that both BR and LR described essentially the same anomaly, i.e. tree rings with tracheids showing a lack of complete cell lignification. Further, Matisons et al. (2019) equated BR with early frost in late summer.

## 1.2. Tree rings and volcanic eruptions in 536 and 1965 CE

In this paper, both BR and FR in *P. longaeva* were analyzed focussing on two periods centered on 536 and 1965 CE (hereafter all dates will refer to the Common Era unless otherwise specified). The period centered on 536 is central to the Dark Ages Cold Period

(410–775, Helama et al., 2017) and to the recently described Late Antique Little Ice Age (536–660; Büntgen et al., 2016). Major volcanic eruption signatures identified in high-resolution ice-core records of volcanic sulfur were reported during the mid-6th century in 536 and 540. This is thought to have caused global low irradiance, climatic cooling and major societal impacts (Larsen et al., 2008; Sigl et al., 2015; Büntgen et al., 2016; Helama et al., 2018; Newfield, 2018). Toohey et al. (2016) indicated that the combined impact of the 536 and 540 volcanic eruptions was unprecedented in the last 1200 years leading to mean temperature anomalies of more than  $-2^\circ\text{C}$  in the Northern Hemisphere. While uncertainties remain regarding the origin of these volcanic eruptions, the El Chichón volcano (Mexico; Nooren et al., 2017) and the Ilopango volcano (El Salvador; Dull et al., 2019) were identified as the potential source for the 540 tropical eruption. The societal impacts of the 536 and 540 eruptions are a subject of ongoing debate. Some emerging criticism has focused on environmental determinism and potentially too large a role attributed to the volcanic eruptions when assessing the cultural volatility of the 6th century (Haldon, 2016; Moreland, 2018).

Tree-ring indicators suggest the existence of global-scale temperature anomalies centered on 536 (see review by Newfield, 2018) as indicated by the formation of FR in trees growing in high-altitude regions in northern hemisphere. Helama et al. (2019) recently reported a FR dated to 536 in the latewood of subfossil *P. sylvestris* trees from Finish Lapland. Using stable carbon isotopes to model solar radiation, Helama et al. (2018) reported an irradiance decline for 536 and 541–544 attributing these negative departures to volcanic dust veil. At high-latitude sites from southern Siberia, Churakova (Sidorova) et al. (2014) reported FR dated to 536 in the latewood of larch trees. The major cooling around 536 was also supported by measurements of ring width, cell-wall thickness, and stable carbon ( $\delta^{13}\text{C}/\delta^{12}\text{C}$ ) and oxygen ( $\delta^{18}\text{O}/\delta^{16}\text{O}$ ) isotope ratios in cellulose (Churakova (Sidorova) et al., 2014). In 536, the observed reduction in ring width and cell wall thickness as well as the strong decline in  $\delta^{13}\text{C}$  and  $\delta^{18}\text{O}$  values all supported the existence of a major cooling of air temperature during the growing season. In the same year, FR were also observed in the mid-earlywood of Siberian pine (*Pinus sibirica* Du Tour) trees growing at the Mongolia timberline (D'Arrigo et al., 2001). At upper forest border bristlecone pine sites in the western United States, LWFR have also been reported in 536 in numerous trees (Brunstein, 1995, 1996; Salzer and Hughes, 2007).

Many of the FR years identified by LaMarche and Hirschboeck (1984), Hallman (2001) and Salzer and Hughes (2007), including 536 and 1965, have been linked to volcanic eruptions. Brunstein (1995) also mentioned that LR and FR co-occurred in *P. aristata* trees in these two years. The 1965 LWFR is thought to be associated with the Mount Agung eruption (Indonesia) in 1963–64 (LaMarche and Hirschboeck, 1984). LaMarche (1970) associated this anomaly with a delayed and cool growing season with sub-freezing temperature at upper treeline elevations in mid-September in Nevada. In this case, cooler than average summers delayed both the onset and the completion of cambial activity rendering trees more susceptible to end of season damaging frosts (LaMarche and Hirschboeck, 1984). Modern (1900–1992) LWFR in *P. aristata*, similar in appearance to those identified in 536, have also been linked to cold growing seasons in Colorado, with record subfreezing temperature in early to mid-September in Colorado as well as severe outbreaks of cold air across the western United States in 1965 from June to September ( $1.5\text{--}2.0^\circ\text{C}$  cooler than normal; Brunstein, 1996). The seasonal timing of the formation of LWFR and BR in *P. longaeva* has also been recently reinforced by xylogenesis studies of *P. longaeva* trees growing in the Great Basin (3355 m a.s.l.). This

work indicates that the onset of xylem formation generally started in early June (mean air temperature reaching  $\sim 7$  °C) with tracheid maturation being completed by mid-September (Ziaoc et al., 2016b).

In dendroclimatology, linking tree-ring features to large-scale circulation has a long tradition. In their review, Hirschboeck et al. (1996) stated that both dendroclimatology and synoptic climatology have had a parallel and interconnected development. Synoptic dendroclimatology aims at connecting “extreme” climate events recorded in tree rings to large-scale circulation by using techniques such as indexing, correlation fields and composite maps (Hirschboeck et al., 1996). Composite maps were used by Stahle (1990) to summarize the conditions involved in the development of weather systems leading to false springs and EWFR formation in post oak (*Quercus stellata* Wangen.) trees growing in the southern Great Plains of the United States. Early growth resumption (false spring) was found to be a major component associated with the formation of EWFR and false springs were often observed during strong La Niña conditions. Hadad et al. (2019) also reported that EWFR in chihuén (*Araucaria araucana* (Molina) K. Koch) trees from Argentina were more abundant in La Niña events which correspond to earlier spring in South America. Composite maps provided evidences that sub-freezing events in Argentina were associated with an anomalous trough crossing the region at 500 hPa in NW–SE direction. Hadad et al. (2020) also showed that earlywood FR in black spruce (*Picea mariana* (Mill.) B.S.P.) trees growing in interior North America were associated with early spring which corresponded to the prevalence in April of a high-pressure system over central Canada. The authors also discussed the influence of the El Niño–Southern Oscillation (ENSO) in being related to the occurrence of false springs in interior North America.

Hirschboeck et al. (1996) analyzed the atmospheric circulation associated with the 1965 LWFR in subalpine bristlecone pine in several localities from the western United States. The authors found that, at both monthly and daily scales, the 1965 LWFR was linked to the development of a strong ridge over the Gulf of Alaska leading to a deep trough located over the western United States and conveying Arctic air masses. In the Colorado Rockies, composite maps indicated that both earlywood and latewood FR in *P. aristata* occurred during amplified mid-to high-latitude atmospheric circulation regimes resulting in cold surface air temperatures penetrating into the westcentral United States (Barbosa et al., 2019). Tardif et al. (2011) established that LR formation in jack pine trees growing in central Canada corresponded to cool summer temperature anomalies across wide areas of interior North America ranging as far as from Minnesota, United States, to the Baffin Island, Canada. Persistent positive height anomalies (ridges) over the Gulf of Alaska and negative height anomalies (troughs) east of the Hudson Bay, as revealed by 500-hPa geopotential heights composite maps, were associated with the LR formation. Hirschboeck et al. (1996) concluded that FR, despite being linked to short-term events (sub-freezing temperature), also contained climate information at a longer time scale making them an excellent proxy from which to evaluate anomalous circulation patterns. Blue rings like FR and LR are also likely linked to specific large-scale components of atmospheric circulation.

### 1.3. Objectives

The objectives of this study were i) to quantify both BR and LWFR in high-elevation *P. longaeva* trees from a wood anatomy perspective, ii) to discuss their presence in relation to climate and atmospheric circulation and iii) to assess their co-occurrence along an elevation gradient in the two time periods discussed above. One

overall goal was to assess if threshold temperatures or particular climate conditions can be associated with BR and FR formation in the second-half of the 20th century so as to provide an analogue for their past occurrence. This research also contributes to discussion surrounding what has been referred to as the fine-scale spatial sensitivity in tree-ring climate response near the upper treeline (Bunn et al., 2011; Bunn et al., 2018; Salzer et al., 2013; Salzer et al., 2014; Tran et al., 2017).

## 2. Methods

### 2.1. Study area

The study area is Pearl Peak at the southern end of the Ruby Mountain Range (Fig. 1). It is located in northeastern Nevada (40.235 N. Lat., 115.542 W. Long.) within the Great Basin physiographic section of the Basin and Range Province of North America. Three tree-ring sites from Pearl Peak were used (PPL, 2996–3086 m; PPU, 3094–3221 m; and PRL, 3074–3291 m). These can be considered separate groves of trees or distinct areas within the upper treeline zone of Pearl Peak. See Salzer and Hughes (2007), Salzer et al. (2009), Salzer et al. (2013) and Bruening (2016) for further information regarding research that used this study location. These three sites were used because initial examinations of specimens from Pearl Peak revealed the existence of many FR in the trees from the upper treeline zone. For the 536

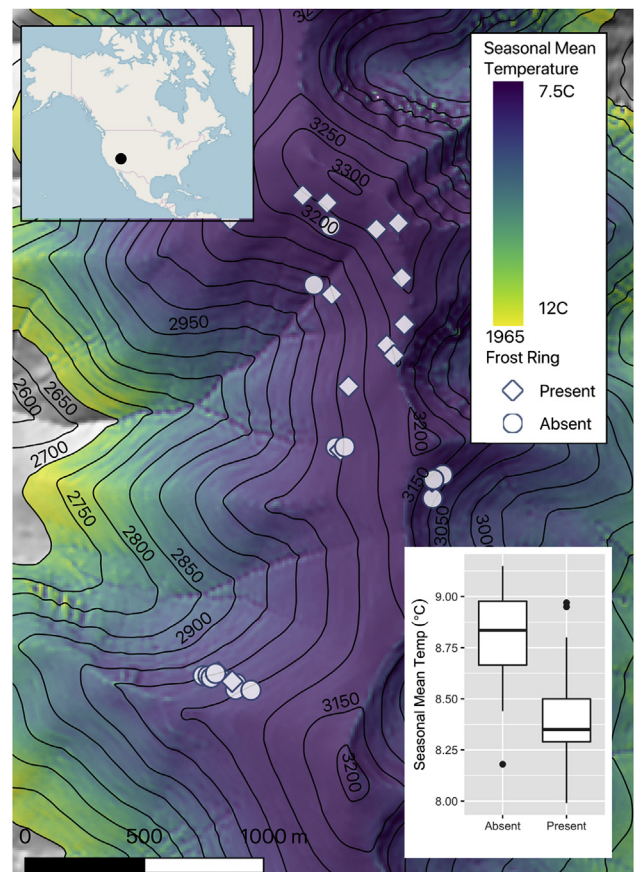


**Fig. 1.** Map of the study area. Upper left inset shows position of study area within North America (black circle). Topographical map indicates location of *Pinus longaeva* trees recording a latewood frost ring in 1965 in relation to derived topoclimate seasonal mean temperature (upper right inset; see section 2.4.2 for details). The lower right inset indicates mean temperature differences between tree locations for those recording the 1965 frost ring and those that did not.

period.

All the samples that were available were used for that temporal interval and for which we were able to effectively cut a thin section for BR analysis. For the 1965 period the same constraint applied; all the living tree core samples along the elevational gradient were used and for which thin sectioning could be done without destroying the core.

## 2.2. Sample collection

The tree-ring samples used in this study were collected over a twelve-year period from 2003 to 2014 as part of an ongoing research effort that uses *P. longaeva* as a paleoclimate proxy record (Salzer and Hughes, 2007; Salzer et al., 2009; Salzer et al., 2013; Tran et al., 2017; Bunn et al., 2018). Core samples from both living *P. longaeva* trees and from remnant wood pieces were used as well as small, hand-sawn samples from remnants. The living tree core samples used in the analyses of 1965 anomalies were roughly distributed along an elevation gradient (Fig. 1). For the 536 period, the 12 *P. longaeva* trees used were more evenly distributed elevationally, growing at a mean elevation of 3225 ( $\pm 47$  m asl). They had an average minimum age of 1150 ( $\pm 619$  years). The 31 trees covering 1965 were growing at a lower elevation, 3126 ( $\pm 92$  m asl) and were younger, with an average minimum age of 554 ( $\pm 336$  years).

## 2.3. Tree-ring anatomy and image analysis

Wood anatomical slides were produced from dried *P. longaeva* cores and cross-sections using a sledge microtome (AO Spencer NO. 860). Continuous thin sections were obtained for each sample either corresponding to the period centered on 536 or 1965. In total, 12 (536) and 31 (1965) tree samples were thin-sectioned. All thin sections were prepared following standard methods (Gärtner et al., 2015; Tardif and Conciatori, 2015). Prior to thin-sectioning, core samples were softened by applying water with a brush and approximately 16–18  $\mu\text{m}$  thin sections were produced after applying a starch-based non-Newtonian fluid (Schneider and Gärtner, 2013) and a water soluble glue (Mowiol 4–88 polyvinyl

alcohol powder; Gärtner et al., 2015). A double-staining procedure (mixture of 1 g safranin and 0.5 g of Astra blue each in 100 ml of distilled water and 2 ml of acetic acid) was applied. The thin sections were soaked in the mixture for a 3–5 min treatment and then rinsed with distilled water to remove excess dye. The sections were next placed in successive ethanol baths (50%, 75, 95% and 99.5%) for 1–2 min and then placed in clearing solvent (Safeclear II) for 1–2 min to clear them of remaining impurities prior to permanently mounting on standard microscope slides. After the anatomical slides were dried, they were visually scanned under a microscope to determine the occurrence of both BR and FR along the exactly annually dated tree-ring sequence (Fig. 2) and the BR and FR data were compiled.

Wood anatomy parameters were generated using image analysis of the 536 and 1965 tree rings. Twelve samples were analyzed for year 536 and 27 samples for year 1965 (four were dropped because of poor condition). The procedures used to measure tracheid dimensions were similar to those described in Waito et al. (2013). The prepared surfaces were photographed with a Nikon DS-Fi1 digital camera connected to a Nikon Eclipse 200 microscope to generate color images at a 20x magnification and a resolution of 2560 x 1920 pixels. A Nikon blue microscope filter was used to increase the contrast between tracheid walls and the lumen. Adobe Photoshop Elements (Ver 14.1) was used to merge images when necessary. Each image was then analyzed using software program WinCELL Pro V 2016c (Régent Instruments Inc. Canada). Correction of images, if needed, mainly involved increasing contrast between the tracheid lumen and cell wall boundaries and visually repairing damage to the tracheid cell walls that resulted from thin sectioning. Despite using a non-Newtonian fluid and a water soluble glue during thin section preparation, sectioning BR and LWFR with a microtome may be challenging due to the presence of under-lignified tracheids. Numerous slides for each sample were thus produced.

For each image, tracheid dimensions were measured along three radial files selected from the upper, middle, and lower portion of the image. The main criterion in selecting the three radial files was that they have minimal artefacts from slide preparation. Tracheids measured along the radial files were divided into an earlywood

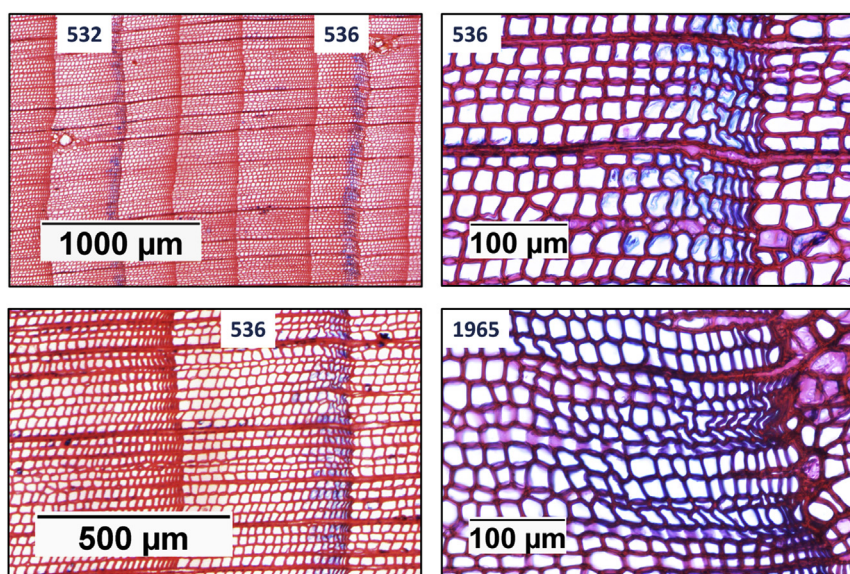


**Fig. 2.** *Pinus longaeva* samples showing both blue rings and frost rings in years 532, 536 or 1965 CE. All pictures come from different trees except that of the bottom left and upper right which came from the same tree and were respectively taken using a Nikon dissecting microscope SMZ1000 and a Nikon compound microscope Eclipse E200. (For interpretation of the references to color in this figure legend, the reader is referred to the Web version of this article.)

(EW) and latewood (LW) component using the average cell wall/lumen ratio  $>0.25$ . This tracheid classification (Mork's definition) however does not consider the wide variability in tree-ring structure associated with the study of tree-ring anomalies (Park et al., 2006) and a manual correction was applied when appropriate. In addition, each tracheid was also visually classified as being a BR or a LWFR tracheid. The tracheid features that were measured included number of tracheids (NT), lumen area [LA], radial lumen diameter [LD], average cell wall thickness [CWT; calculated as half the shared cell wall with the tracheid preceding and that following the tracheid being measured along the radial file] and the wall-to-tracheid ratio [WTR; calculated as CWT/LD]. This resulted in five anatomical parameters for the earlywood (EW), the latewood (LW) and for tracheid classified as BR and FR. The proportion of earlywood (EW%), latewood (LW%), blue ring (BR%) and frost ring (FR%) tracheids was also calculated. For each sample, the average of the three radial files was calculated resulting in a total 24 anatomical parameters for each of the 536 (12 trees) and 1965 (27 trees) tree rings.

## 2.4. Statistical analyses

### 2.4.1. Tree-ring anomalies and climate

To evaluate the association between the frequency of tree-ring anomalies (BR and FR) and synoptic circulation, composite maps were made using the Climate Explorer facility (<http://climexp.knmi.nl/>; Trouet and van Oldenborgh, 2013) of the Royal Netherlands Meteorological Institute (KNMI). Composite maps are particularly useful when derived from non-continuous, event-based time series (Hirschboeck et al., 1996; Trouet and van Oldenborgh, 2013). Composite maps were derived using the NOAA-CIRES-DOE Twentieth Century Reanalysis (V3) monthly geopotential heights (HGT, in mpp) at 500 hPa level and in a global regular  $1.0^\circ \times 1.0^\circ$  latitude-longitude grid was used (Slivinski et al., 2019; NOAA/OAR/ESRL PSL, Boulder, Colorado, USA, <https://psl.noaa.gov/>). The objective was to identify and to compare dominant synoptic-scale circulation patterns associated with BR and FR formed during the period centered on 1965. The analyses were conducted over the period 1954–2006 which corresponded to the period when a minimum of ten trees were included in the tree-ring anomaly chronologies. To calculate the association with "local" climate, mean of monthly minimum and maximum temperature and total precipitation data were obtained for the grid pertaining to Pearl Peak (40.235 N. Lat. and 115.542 W. Long; Spatial resolution 4 km, PRISM Climate Group, Oregon State University, <http://prism.oregonstate.edu>, created 18 Oct. 2019). All correlation analyses between frequency of tree-ring anomalies (BR and both earlywood and latewood FR) and gridded climate data were done using Spearman's rho correlation due to the non-normal distribution of the 1954–2006 tree-ring anomalies. To complement the correlation analyses, we also tested for differences in mean monthly temperatures using the non-parametric Mann-Whitney U tests.

Because there are no long-term weather stations for the study area, we used atmospheric air temperatures at 500 mb height from the NOAA-CIRES-DOE 20CR V3 (Slivinski et al., 2019) from 1836 to 2015 to put BR and LWFR formations into a longer-term context. To better approximate temperature experienced by the trees we used daily interpolated surface temperature data PRISM (Daly et al., 2008) from 1982 to 2015 to adjust the NOAA-CIRES-DOE 20CR V3 data. Because these two data sets covary strongly, we modeled the surface temperature from PRISM using the reanalysis data to create a surface temperature from 1836 to 2015. We used a generalised least squares of the form  $y_t = \beta_0 + \beta_1 x_t + \epsilon_t$  where  $t$  is the time in days,  $y$  is the PRISM data,  $x$  is the NOAA-CIRES-DOE 20CR V3 data,

$\beta_0$  and  $\beta_1$  are coefficients and  $\epsilon$  are autocorrelated residuals following an ARMA (1,2) process. This model had an  $R^2$  of 0.83. Extending the surface temperature in this way allows us to put the years with abundant LWFR and BR into a longer-term context.

### 2.4.2. Tree-ring anomalies and environmental features

The environmental and climate setting between trees recording BR only, LWFR only and both BR/LWFR (recording trees) as compared to co-located trees without these anomalies (non-recording trees) was examined using non-parametric Mann-Whitney U tests. First, we tested for differences in tree elevation in 536 ( $n = 12$ ), 1965 ( $n = 31$ ) and 1978 ( $n = 29$ ). In addition, topoclimate variables were derived for each tree location. Given that topography affects local climate at scales relevant to tree-ring formation (e.g. see Bunn et al., 2011), we tested to see if trees growing in cooler topographic locations might be more susceptible to record anatomical growth anomalies driven by colder temperatures as compared to trees in surrounding areas.

At Pearl Peak, Bruening (2016) and Bruening et al. (2017, 2018) used 50 temperature sensors arrayed across topographic gradients to model monthly temperature anomalies with topography ("topoclimate") at a 10-m horizontal resolution. Those data, and data from other Great Basin treeline sites, showed that topography attenuates maximum and minimum air temperatures beyond the expectations derived from elevational-lapse rates. In particular, Bruening et al. (2017) found that temperatures during the growing season vary according to topographic setting several times more than predicted by the dry adiabatic lapse rate. These observations have helped to explain variations in the position of the alpine treeline on the landscape (Bruening et al., 2017, 2018) as well as the growth response of individual trees (Tran et al., 2017; Bunn et al., 2018). We used four topoclimate variables developed by Bruening et al. (2017, 2018) to assess if BR and LWFR were recorded in trees in colder topoclimate settings than generally found even at the alpine treeline ecotone. These variables were mean temperatures in May and in September (respectively start and end of growing season), the length of growing season in days (LGS) defined as the sum of days with daily mean temperature above  $0.9^\circ \text{C}$ , and the seasonal mean temperature in  $^\circ \text{C}$  (SMT) (Körner, 2012). SMT was defined as average of the daily mean temperatures for the days included in the LGS. These topoclimate variables were calculated following Bruening (2016), Bruening et al. (2017), and Tran et al. (2017) for each tree location, provided a way of integrating the deviation in temperature that a given tree experiences over the growing season.

### 2.4.3. Tree-ring anatomy of blue and latewood frost rings

To determine if the anatomical features in tree rings (EW and LW) differed significantly between recording (BR only, LWFR only and both BR/LWFR) and non-recording trees the non-parametric Kruskall-Wallis one-way analysis of variance was used. The Dunn-Bonferroni post-hoc method was performed following a significant Kruskal-Wallis test. Both year 536 ( $n = 12$ ) and 1965 ( $n = 27$ ) were pooled in this analysis. Additionally, to determine if BR tracheid features differed from LWFR ones, the Mann-Whitney U Test was performed.

Standardized tracheidograms were also produced to compare yearly tree-ring anatomical profiles (Vaganov 1990; Gindl, 1999; Vaganov et al., 2006; Ziaco et al., 2014a; Ziaco et al., 2014b). Tracheidograms represent measurement profiles of tracheid dimensions across tree rings. Standardization allows for structural comparison of rings with a different number of cells (Vaganov et al., 2006). Yearly anatomical features (LA, LD, CWT and WTR) were computed using the "tgram" package (DeSoto et al., 2011; available

from CRAN; <https://cran.r-project.org>) in R (R Core Team, 2013). The tracheidograms for year 536 and 1965 were standardized to 20 cells which closely matched the average number of tracheids observed in the 1965 samples. This analysis allowed comparisons of tracheid dimensions for the year 536 and 1965 and of tree rings recording and not recording BR and FR. All standardized tracheidograms (536: n = 36 radii pertaining to 12 trees and 1965: n = 81 radii pertaining to 27 trees) were averaged to produce mean tracheidograms.

### 3. Results

#### 3.1. Blue rings and frost rings: their frequency and climatic connection

In the mid-6th century both BR and LWFR were abundant in 532 and 536 and to a lesser extent in 574 and 525 (Fig. 3a). We also observed a cluster of BR from 539 to 542 with a maximum observed in 540. Few EWFR were observed and years with solely a BR being recorded were more abundant than for the second half of the 20th century (Fig. 3b). In the latter period, both BR and LWFR were recorded in high abundance in 1965 and 1978 and to a lesser extent in 1982. Earlywood FR never reached the same abundance as LWFR and were not synchronized with BR. In contrast, LWFR years and BR were synchronized; BR were typically observed in LWFR years.

Data from individual trees (not presented) indicated that, within a tree, LWFR were almost always associated with a BR, whereas tree rings showing only a BR or only a LWFR were less common. At the tree level and specifically looking at years 536 and 1965, of the recorder trees (10/12 and 18/27 respectively), most trees that recorded a BR also produced a LWFR (6/10, 12/18 respectively); few trees recorded solely a BR (3/10, 4/18 respectively) or a LWFR (1/10, 2/18 respectively). Chi-square testing for 1965 indicated that BR and LWFR were not independent and trees with BR recorded more LWFR than expected by chance (Pearson Chi-Square

value = 811.519, p = 0.001, n = 31).

Correlating the portion of the chronologies pertaining to a minimum of 10 trees (1954–2006; Fig. 3b) with PRISM gridded climate data further supported the similarities between BR and LWFR in contrast to EWFR (Fig. 4). Earlywood FR were negatively correlated to March precipitations and positively to May maximum temperatures (Fig. 4). In contrast, both LWFR and BR were found to be more frequent in years characterized by cooler minimum temperature in late spring months (May and May–June; Fig. 4a). Blue ring and LWFR were also found to be more frequent in years when maximum temperatures were cooler in the late growing season (August–September) as well as during the entire growing season (Fig. 4b). Compared to BR, LWFR had slightly stronger negative correlation with minimum temperatures. The Mann-Whitney U test confirmed that the mean of May maximum temperatures was significantly warmer (by 2 °C) in years forming EWFR (Suppl. Tables 1 and 2). In contrast, years with LWFR and BR recorded significantly cooler minimum temperatures in May (1.5 and 1.4 °C respectively) with LWFR years also recording significantly cooler minimum temperatures throughout the growing season. Years with LWFR and BR also recorded significantly cooler maximum temperatures during the growing season and in particular in the late portion of the growing season (Suppl. Tables 1 and 2). Further both the modeled surface daily temperature data for 1965, 1978 and 1982 (Fig. 5) and the 500 mb daily temperature data (not presented) clearly indicated that in these three years much of May, June and September fell below the long-term temperature average. Major sub-freezing temperature departures were also observed in September (Fig. 5); these presumably being the source of the frost damages at ground level.

At the hemispheric scale, the synoptic signal associated with EWFR was coherent with the Spearman's rank correlation analyses and composite maps indicated that in EWFR years a high ceiling (Great Basin High) in May prevailed over the study area (Fig. 6). The signal associated with both BR and LWFR anomalies was coherent

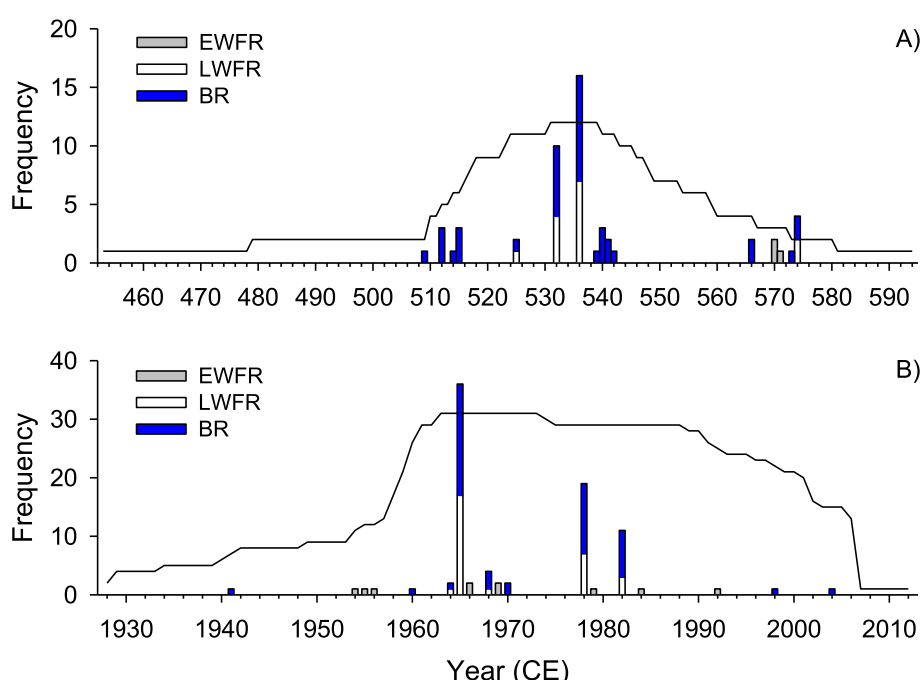


**Fig. 3.** Distribution of earlywood frost rings (EWFR), latewood frost rings (LWFR) and blue rings (BR) in *Pinus longaeva* trees within the 536 (A) and 1965 (B) CE periods. The number of samples is indicated by the solid line. (For interpretation of the references to color in this figure legend, the reader is referred to the Web version of this article.)

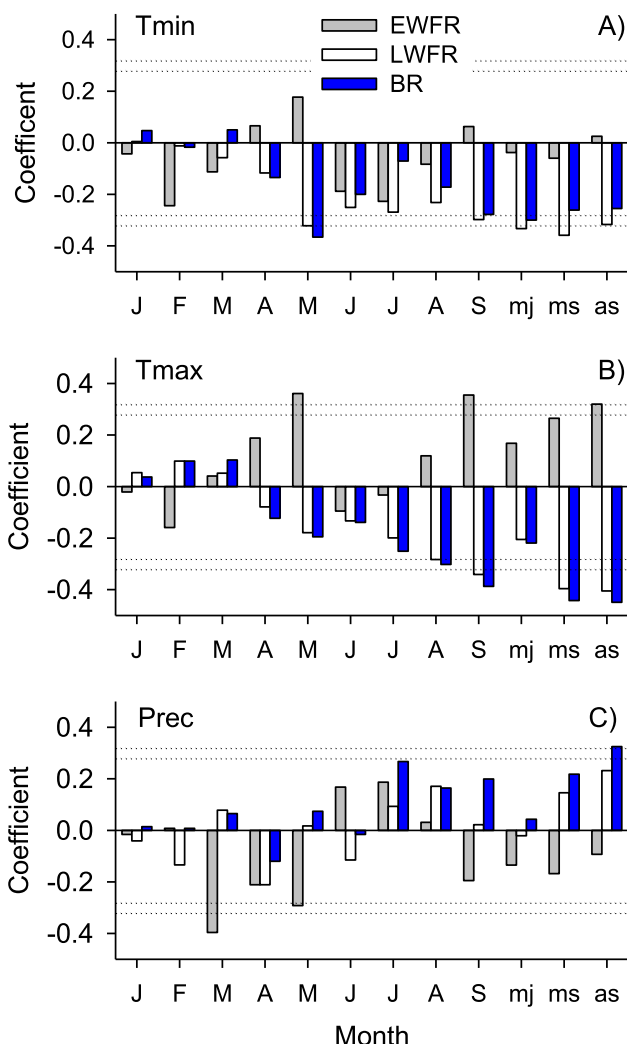


**Fig. 4.** Spearman rank correlation coefficients between earlywood frost rings (EWFR), latewood frost rings (LWFR), blue rings (BR) chronologies and PRISM climate variables for the period 1954–2006. The dotted lines indicate significant correlation at  $p < 0.05$  and  $p < 0.01$ . Capital letters indicate months from January to September. mj: May and June average, ms: May to September average and as: August and September average. (For interpretation of the references to color in this figure legend, the reader is referred to the Web version of this article.)

over a large portion of North America with composite maps showing negative that both BR and LWFR were more common during years when the growing season was characterized by a low pressure system (Great Basin Low) persisting from May to September (Fig. 6). These results indicate that during BR (LWFR) years, mean growing season temperatures were cooler than in non-recording years with significant intrusions of cold air masses over the western portion of the United States. In the month of September, the deep trough over the study area was particularly noticeable in BR years. Inversely, EWFR may be more frequent in years characterized by warm Mays and an early reactivation of cambial activity.

### 3.2. Blue ring, latewood frost ring, elevation and topoclimate

In order to account for BR and LWFR formation in *P. longaeva* trees, we tested for significant differences between tree locations both in elevation and in topoclimate features using years when BR and LWFR were observed in a large number of trees i.e., 536, 1965

and 1978 (Figs. 1 and 3). The results indicated that elevation was most often discriminating among trees recording or not recording a given anomaly (Table 1). In 1965, 1978, a difference of about 100m was observed between recorder and non-recorder trees. This difference in elevation reflects.

Significant cooler seasonal mean temperature and shorter length of the growing season for recorder trees (Fig. 1 and Table 1). For example, in 536, despite a low number of observations ( $n = 12$ ), trees recording LWFR or both BR and LWFR tended ( $p < 0.1$ ) to also grow at higher elevation and to record lower seasonal mean temperatures than those not recording these anomalies. Trees recording anomalies also experience shorter and cooler growing seasons (Table 1).

### 3.3. Anatomy of blue ring and latewood frost rings

Comparing the average tracheid features across anomalies (BR only, LWFR only and both BR-LWFR) using combined data from 536 to 1965 revealed few statistical differences among categories (Table 2). Among them, trees recording both BR and LWFR had earlywood tracheids with both significantly smaller lumen areas and length values than trees that recorded neither BR nor LWFR. The most significant difference however, was observed in the latewood; trees recording both BR and LWFR had latewood tracheids with significantly reduced cell wall thickness ( $p < 0.001$ ; Table 2). In both BR and LWFR, secondary walls in latewood tracheids were 37% less thick than in trees not showing the anomalies. Testing using solely the 1965 data revealed essentially the same results. Comparisons between tracheid features identified as being a constituent of a BR and/or a LWFR revealed no statistical differences between anomalies (Table 3). Both BR and LWFR were composed of about 6 tracheids on average representing about 20% of the ring width.

Given the absence of significant differences in BR and LWFR tracheid features, the tree rings showing BR only and LWFR only were pooled with those showing both anomalies when calculating the standardized tracheidograms calculated for 536 and 1965 (Fig. 7). The standardized tracheidograms indicated, both in 536 and 1965, cell wall thickness was the main variable differentiating tree rings showing anomalies from those not showing anomalies (Fig. 7cd). Starting with a CWT of about 2.5  $\mu\text{m}$ , the year 536 values slightly increased to approximately 3.0  $\mu\text{m}$ . The recording and non-recording trees then diverged (cell 10), with the tree rings presenting anomalies decreasing toward a value of 2.0  $\mu\text{m}$  at the end of the growing season. In 1965, a similar trend was observed with the divergence between recorder and non-recorder trees occurring later in the tree ring. Compared to 536, the lumen area and lumen diameter in 1965 was greater and average cell wall was more similar (Fig. 7abef). Smaller differences were observed in CWT between the two years studied (Fig. 7cd). The reduced lumen area and lumen width in 536 compared to 1965 also led to higher wall to cell ratio observed in 536 (Fig. 7gh).

## 4. Discussion

### 4.1. Frost rings, blue rings and “normal” rings in *P. longaeva*

In this study, EWFR in *P. longaeva* trees were rarely observed compared to LWFR as earlier noted (LaMarche and Hirschboeck, 1984; Salzer and Hughes, 2007). In *P. aristata*, the same point was reported by others (LaMarche, 1970; Brunstein, 1995) with the exception of Barbosa et al. (2019) who specifically selected sites subjected to intense cold air drainage. In numerous studies, EWFR have been associated with late spring frost events following early reactivation of cambial activity in years with warm springs (Stahle,

**Table 1**

Mann-Whitney *U* test indicating significant differences in topographic (Elev: elevation) and topoclimatic (SMT: seasonal mean temperature; LGS: length of growing season in days) variables between trees not recording and recording a tree-ring anomaly (blue ring, frost ring and both) in years 536, 1965 and 1978. The mean and standard deviations are indicated. Note that the number of observations per group varies for each year analyzed. Bold number in shaded grey box indicates significant differences at  $p < 0.05$ .

Year	Variables	NoBR	BR	Pvalue	NoLWFR	LWFR	Pvalue	NoBR-LWFR	BR-LWFR	Pvalue
536	N	3	9	—	5	7	—	6	6	—
	Elev.	3213 ± 12	3230 ± 54	0.482	3203 ± 25	3242 ± 54	0.073	32bb07 ± 24	3244 ± 59	0.065
	SMT <sup>a</sup>	8.4 ± 0.1	8.1 ± 0.2	0.100	8.3 ± 0.1	8.1 ± 0.2	0.073	8.3 ± 0.1	8.1 ± 0.2	<b>0.026</b>
	LGS <sup>a</sup>	148.3 ± 1.2	146.9 ± 5.3	0.482	148.6 ± 2.6	146.3 ± 5.7	0.106	148.7 ± 2.3	145.8 ± 6.1	0.065
	TmeanMay <sup>a</sup>	0.03 ± 0.1	-0.23 ± 1.0	0.482	0.04 ± 0.6	-0.31 ± 1.0	0.268	0.02 ± 0.6	-0.35 ± 1.1	0.240
	TmeanSept <sup>a</sup>	7.4 ± 0.1	7.2 ± 0.4	0.373	7.4 ± 0.1	7.2 ± 0.4	0.202	7.4 ± 0.1	7.1 ± 0.4	0.065
1965	N	12	19	—	14	17	—	16	15	—
	Elev.	3067 ± 76	3162 ± 83	<b>0.003</b>	3071 ± 66	3171 ± 87	<b>0.003</b>	3084 ± 77	3170 ± 87	<b>0.009</b>
	SMT	8.8 ± 0.3	8.5 ± 0.3	<b>0.004</b>	8.8 ± 0.3	8.4 ± 0.3	<b>0.005</b>	8.7 ± 0.3	8.5 ± 0.3	<b>0.024</b>
	LGS	160.9 ± 6.8	153.2 ± 7.6	<b>0.010</b>	161.1 ± 6.0	152.2 ± 7.6	<b>0.002</b>	159.6 ± 6.9	152.5 ± 7.9	<b>0.019</b>
	TmeanMay	1.6 ± 1.0	0.5 ± 1.2	<b>0.010</b>	1.6 ± 0.9	0.4 ± 1.2	<b>0.002</b>	1.4 ± 1.0	0.4 ± 1.2	<b>0.017</b>
	TmeanSept	8.4 ± 0.5	7.8 ± 0.6	<b>0.010</b>	8.4 ± 0.5	7.7 ± 0.6	<b>0.003</b>	8.3 ± 0.5	7.7 ± 0.6	<b>0.021</b>
1978	N	17	12	—	22	7	—	23	6	—
	Elev.	3086 ± 76	3190 ± 80	<b>0.003</b>	3106 ± 84	3203 ± 83	<b>0.028</b>	3112 ± 88	3194 ± 86	0.090
	SMT	8.7 ± 0.3	8.4 ± 0.3	<b>0.011</b>	8.6 ± 0.3	8.4 ± 0.3	<b>0.037</b>	8.6 ± 0.3	8.4 ± 0.3	0.080
	LGS	159.0 ± 6.9	151.1 ± 7.7	<b>0.016</b>	157.6 ± 7.7	149.7 ± 6.7	<b>0.028</b>	157.1 ± 7.9	150.3 ± 7.1	0.090
	TmeanMay	1.4 ± 1.0	0.2 ± 1.2	<b>0.009</b>	1.1 ± 1.2	0.1 ± 1.0	<b>0.032</b>	1.0 ± 1.2	0.2 ± 1.1	0.090
	TmeanSept	8.2 ± 0.5	7.6 ± 0.6	<b>0.021</b>	8.1 ± 0.6	7.5 ± 0.5	0.055	8.1 ± 0.6	7.6 ± 0.6	0.142

<sup>a</sup> Topoclimate data from [Bruening \(2016\)](#).

**Table 2**

Kruskall-Wallis one-way analysis of variance among cell features pertaining to tree rings showing or not tree-ring anomalies. The data was generated from 39 bristlecone pine trees and includes tree rings produced in 536 (n = 12) and in 1965 (n = 27). Bold number in grey box indicates significant test with significant ( $P < 0.05$ ) Dunn-Bonferroni post-hoc test indicated by different small case letters.

	Variables	No BR-LWFR	BR only	LWFR only	BR-LWFR	Pvalue
EW	N (536,1965)	11 (2, 9)	7 (3, 4)	3 (1, 2)	18 (6, 12)	—
	Tracheid No	14.81 ± 8.37	18.33 ± 16.04	14.22 ± 2.55	21.39 ± 15.60	0.635 <sup>a</sup>
	%	91.20 ± 11.20	92.77 ± 4.73	97.34 ± 0.31	95.62 ± 3.60	0.169 <sup>a</sup>
	LA (μm <sup>2</sup> )	503.61 ± 114.72a	420.10 ± 168.72 ab	516.44 ± 20.53 ab	373.74 ± 78.74b	<b>0.016</b> <sup>b</sup>
	LD(μm)	23.27 ± 2.83a	20.95 ± 3.54 ab	25.08 ± 1.96a	20.07 ± 2.02b	<b>0.003</b> <sup>b</sup>
	CWT (μm)	2.72 ± 0.38	2.74 ± 0.47	2.54 ± 0.80	2.41 ± 0.34	0.113 <sup>b</sup>
LW	CWR (%)	0.13 ± 0.03	0.14 ± 0.04	0.12 ± 0.5	0.13 ± 0.02	0.706 <sup>a</sup>
	Tracheid No	2.42 ± 2.00	2.81 ± 1.45	1.00 ± 0.33	2.06 ± 1.46	0.153 <sup>a</sup>
	%	8.80 ± 11.20	7.23 ± 4.73	2.66 ± 0.30	4.38 ± 3.60	0.169 <sup>a</sup>
	LA(μm <sup>2</sup> )	114.07 ± 32.12	91.77 ± 39.55	116.48 ± 23.44	79.93 ± 44.29	0.126 <sup>a</sup>
	LD(μm)	6.08 ± 1.71	5.46 ± 1.95	6.80 ± 2.89	4.17 ± 2.19	0.123 <sup>a</sup>
	CWT (μm)	2.76 ± 0.43a	2.38 ± 0.35 ab	2.70 ± 0.33 ab	1.74 ± 0.79b	<b>0.001</b> <sup>b</sup>
	CWR (%)	0.69 ± 0.29	0.68 ± 0.32	0.86 ± 0.41	0.66 ± 0.40	0.819 <sup>a</sup>

<sup>a</sup> Also not significant ( $p < 0.05$ ) using data for year 536 and 1965 separately.

<sup>b</sup> Also significant ( $p < 0.05$ ) using data from 1965 only.

1990; [Montwé et al., 2018](#); Hadad et al. 2019, 2020). Here, maximum temperatures in May (corresponding to a Great Basin high at 500 Mb) were positively associated with EWFR formation supporting previous findings that early cambial reactivation increases the probability that trees experience and record late spring frosts. Despite their low abundance, EWFR were observed more frequently in the 20th-century period compared to the 6th-century period. In contrast to EWFR, LWFR have been associated with both a delayed start of cambial activity and a cooler than average growing season delaying tracheid maturation, thus increasing the risk of frost damages in the late growing season ([LaMarche and Hirschboeck, 1984](#); [Brunstein, 1996](#); [Montwé et al., 2018](#)).

Latewood FR were often associated with the same individual or other nearby trees recording BR in the same year. In contrast, BR were often recorded without a corresponding LWFR being recorded. This indicates that cool growing seasons were not always associated with cold air intrusions leading to sub-freezing temperatures in the late growing season and the formation of LWFR. The lack of independence between BR and LWFR years suggests that both anomalies result as a response to the same or a very similar cause: A climatic system that generates cool late springs,

cool summers and cool early falls. In these years, the location of a tree with regard to the topographical gradient (mainly elevation) determines which *P. longaeva* trees will record a BR, punctuated or not by a LWFR, i.e., if prolonged sub-freezing temperatures are encountered. Our results support previous findings indicating that LWFR are associated with years with a cool late spring, a cool summer and a cool early fall ([LaMarche and Hirschboeck, 1984](#); [Brunstein, 1996](#); [Barbosa et al., 2019](#)). The weather conditions leading to the LWFR of 1965 have been well described ([LaMarche and Hirschboeck, 1984](#); [Brunstein, 1996](#); [Barbosa et al., 2019](#)) and will not be further discussed.

Our results also indicated a lack of significant differences between tracheid features measured in BR and LWFR years except that the latter clearly showed macroscopic damages resulting from late growing season frosts at the time tracheids are differentiating. The frost events leading to LWFR may also have prevented normal subsequent tracheid differentiation, thus accentuating the presence of under-lignified tracheids. Generally, a band of under-lignified and crumpled tracheids is observed as part of a FR ([Glerum and Farrar, 1966](#)). In Monterey Pine (*Pinus radiata* (D. Don)), [Donaldson \(1992\)](#) also noted poor differentiation of

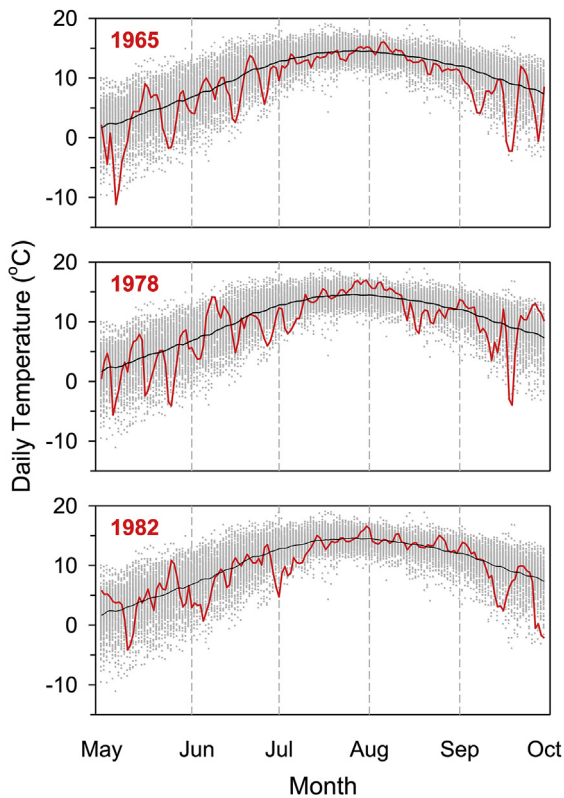


**Fig. 5.** Modeled surface daily temperatures from May 1st 1836 to September 30th 2015 (see section 2.4.1 for details). The black line is the daily mean for the entire period and the red lines indicate the years 1965, 1978 and 1982 (top to bottom). Note the severe September freezing episodes in 1965 and 1978. (For interpretation of the references to color in this figure legend, the reader is referred to the Web version of this article.)

latewood tracheids associated with FR formation. In this study, latewood secondary wall thickness in both BR and LWFR years differed significantly from years with “normal” tree rings and the comparative tracheidograms produced were similar to those found in LR studies (Gindl, 1999; Gindl and Grabner, 2000). The same general departure in latewood cell wall thickness was observed when compared to “normal” tree rings with no differences in lumen diameter. Unfortunately, no previous BR studies to our knowledge have provided tracheid cell wall measurements.

In *P. longaeva*, BR looked very similar to the incompletely differentiated latewood tracheids described in silver fir (*Abies alba* Mill.) by Gričar et al. (2005; Fig. 1). Their samples collected in early autumn (October 17th) presented blue-stained inner latewood wall parts which were absent in samples collected in late autumn (November 14th) which showed complete tracheid differentiation. In *P. longaeva*, BR also look similar to the unspecified BR observed in the latewood of *P. aristata* (Barbosa et al., 2019, Fig. 2). The BR in *P. longaeva* were also similar to some photographs of BR in *P. nigra* provided by Crivellaro et al (2018, Fig. 1) and in which the under-lignified portion of the tracheid cell wall was mainly restricted to the inner portion of the wall. *Pinus longaeva* BR also appear to be more lignified than those presented in *P. nigra* (Piermattei et al., 2015) in which solely the cell corners were lignified indicating a premature interruption of lignification. We did not observe lignification occurring solely in the tracheid corners. Typically, tracheid lignification begins at the cell corners in the middle lamella and S1 regions, eventually spreading across the secondary wall towards the lumen after the formation of the S2 and S3 layers (Donaldson, 1992).

#### 4.2. Blue rings and pale latewood (light) rings

Our results strongly suggest that BR and LR are representing the same irregularity, perhaps presenting a gradient in tracheid lignin content or in duration of tracheid differentiation leading to reduced secondary wall thickness. Both anomalies are associated with cooler growing season temperatures and reduced lignification of latewood tracheids. All published BR studies have identified cool growing season (early, entire or end) temperatures as the main driver for the observed reduced tracheid lignification (Piermattei et al., 2015; Semeniuc et al., 2016; Crivellaro et al., 2018; Montwé et al., 2018; this study). Cool growing seasons have also been associated with the formation of LR in numerous coniferous species (Szeicz, 1996; Gindl and Grabner, 2000; Gindl et al., 2000; Girardin et al., 2009; Tardif et al., 2011; Montwé et al., 2018). Light rings are also characterized by reduced lignification of latewood tracheids (Gindl and Grabner, 2000; Gindl et al., 2000). Interestingly, the abnormally cool growing season conditions of 1965 that caused a BR in *P. longaeva* were similar to those related to 1965 LR formation in jack pine (*Pinus banksiana* Lamb.; Girardin et al., 2009, Fig. 3) in central Canada. Both LR (Brunstein, 1995) and BR (Hughes et al., 2016; this study) have been reported in bristlecone pine trees. Brunstein (1995) defined LR in *P. aristata* as rings with fewer latewood cells than the surrounding rings leading to a narrow latewood ring. He also reported that LR and LWFR were co-occurring in numerous years and he referred to various radii recording either a LR or a LWFR. Similar to our findings, Brunstein (1995) reported that in 536 and in 1965 both LR and LWFR were recorded (BR and LWFR in this study).

It is worth noting that LR are more difficult to detect macroscopically in coniferous species producing thin latewood compared to those producing thick latewood. Among Canadian boreal conifers the demarcation between LR (pale latewood) and thin latewood years is unequivocal in species producing thick latewood (e.g., *P. banksiana* and *Larix laricina* ((Du Roi) K. Koch), whereas identification difficulties arise with species producing thin latewood (e.g., *P. mariana* and *Picea glauca* ((Moench) Voss)). In contrast to boreal pine species, *P. longaeva* trees produce an extremely narrow latewood band. Like in other studies (Baas et al., 1986; Ziaco et al., 2016a) tree-ring width variations in *P. longaeva* were mainly attributable to earlywood tracheids; latewood often being composed of solely one or two cells (Mork's definition of latewood). Given that macroscopically identifying LR can present difficulties in species producing thin latewood, it may prove beneficial, in absence of more easily detectable LWFR, to assess if BR are present. Both BR and LR are proxies for cool growing season temperature with BR providing qualitative information about lignification. It still remains unclear if BR and LR can provide additional climate information compared to quantitative measurement of lignin and/or latewood density. Their observation is however less demanding in terms of costs, time and equipment. When working with species that produce little latewood it can also be challenging to distinguish LR years from thin latewood years. Future quantitative work aimed at deriving the differences between thin latewood rings and pale latewood rings (BR and LR included) in *P. longaeva* may reveal that thin latewood years and LR (BR) years provide different climate information.

#### 4.3. Mid-6th and Late-20th century climate

Regional cool conditions in the 6th century are supported by the observation that our LWFR chronologies concurred with Salzer and Hughes (2007) who identified LWFR in 532, 536 and 574 in *P. longaeva* trees from various mountain ranges in the western

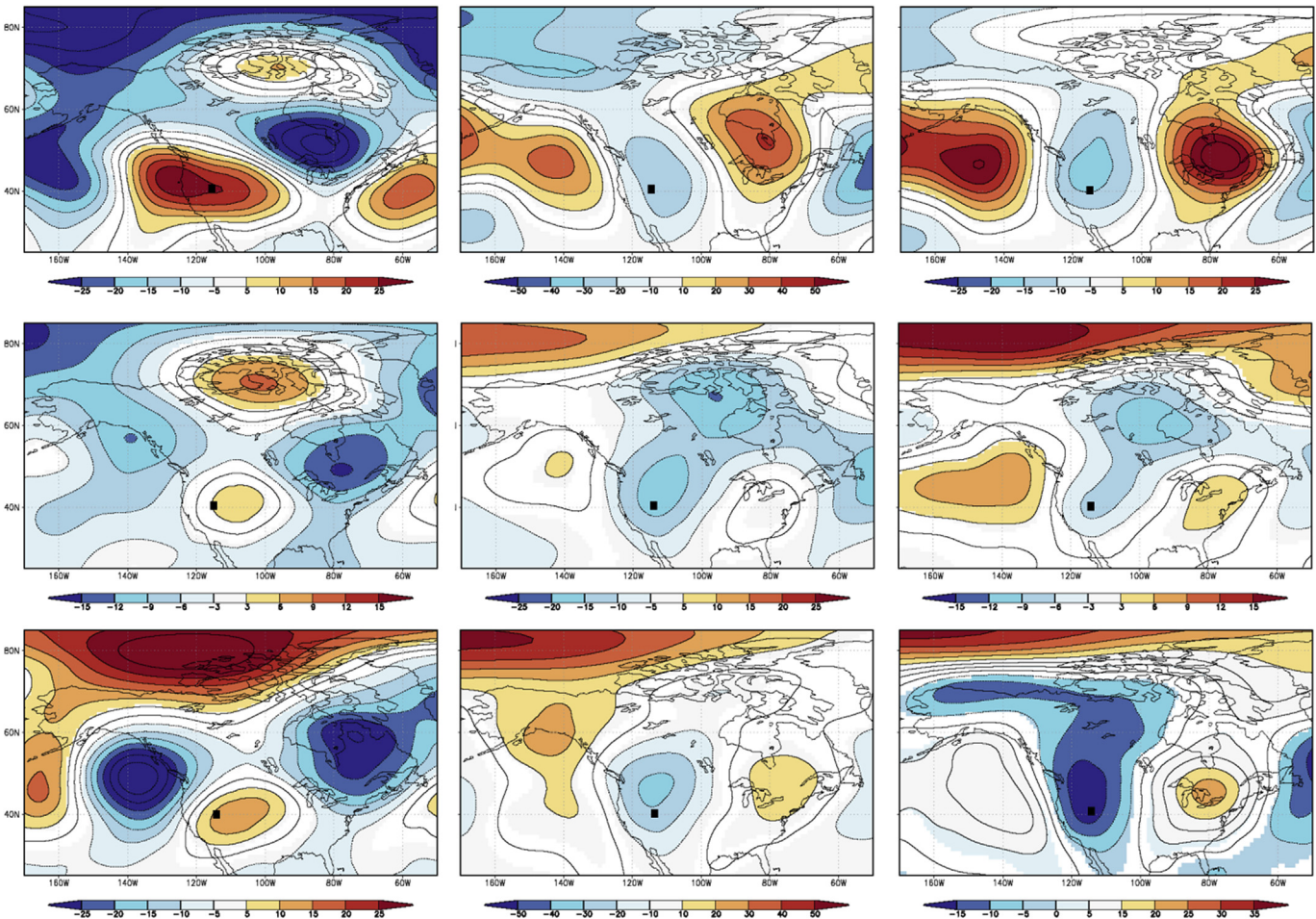


**Fig. 6.** Composite maps derived for years showing earlywood frost ring (left panel), latewood frost rings (middle panel) and blue ring (right panel) chronologies. The maps represent gridded monthly geopotential heights at 500 hPa level from NOAA-CIRES-DOE Twentieth Century Reanalysis (V3; NOAA/OAR/ESRL PSL, Boulder, Colorado, USA, <https://psl.noaa.gov/>) for May (upper), May to September (middle) and September (lower). The period of analysis is 1954–2006. The black square indicates position of the study area. The maps were created using the Royal Netherlands Meteorological Institute (KNMI) Climate Explorer. (For interpretation of the references to color in this figure legend, the reader is referred to the Web version of this article.)

**Table 3**

Mann-Whitney U Test performed between the cell features identified as a blue ring or a frost ring. The data included tree rings produced in 536 and in 1965 and for which tracheids were classified as part of a blue ring or a frost ring.

Variables	Blue Ring	Frost Ring	Pvalue
N	25	21	—
Tracheid No	$6.09 \pm 4.25$	$5.40 \pm 3.56$	0.581
Total Ring (%)	$20.89 \pm 12.71$	$17.69 \pm 7.37$	0.453
Lumen area ( $\mu\text{m}^2$ )	$194.01 \pm 79.21$	$205.39 \pm 72.09$	0.597
Lumen diameter ( $\mu\text{m}$ )	$10.63 \pm 3.25$	$11.22 \pm 3.53$	0.589
Cell wall thickness ( $\mu\text{m}$ )	$2.07 \pm 0.41$	$2.00 \pm 0.41$	0.453
Cell tracheid ratio (%)	$0.38 \pm 0.24$	$0.36 \pm 0.21$	0.843

United States. In our study, a LWFR (and BR) was also observed in 525. Salzer and Hughes (2007) also reported LWFR in 541 in the White Mountains of California. The cluster of BR recorded in 539–542 suggests that cool temperatures prevailed through the growing seasons during this extended interval. In fact, in the trees growing in the mid-6th century more annual rings recorded solely BR (without FR) in contrast to the warmer mid-20th century (Salzer et al., 2009). During the period centered on 1965, more EWFR were observed likely indicating the occurrence of false springs and earlier onset of radial growth and potentially longer growing seasons. The positive association between EWFR and warm May

temperature supports these findings. Tree-ring width (number of tracheids) in the 536 period was also narrower compared to the 1965 period. This reduced radial growth further suggests cooler and shorter growing seasons, although it should be noted that the 536 trees were growing at slightly higher elevation. The tracheid lumen area and lumen diameter were also reduced in tree rings from 536 compared to 1965. Ziaco et al. (2014a) also reported that *P. longaeva* trees growing at higher elevation produced smaller cellular elements. Salzer and Hughes (2007) also observed a ring-with minimum in 536. In addition to the 1941 and 1965 LWFR reported by Salzer and Hughes (2007), we also observed LWFR in 1964, 1978 and 1982.

The formation of LWFR in *P. longaeva* trees has been associated with outbreaks of polar air during the growing season with the formation of a deep mid-tropospheric trough over the western United States (LaMarche and Hirschboeck, 1984; Hirschboeck et al., 1996). These findings are supported by our results. The study area was significantly cooler during years recording BR and/or LWFR (early, entire and late growing season) and results suggest the persistence of troughs over the Great Basin region bringing cold temperatures. A recent study of FR in *P. aristata* (Barbosa et al., 2019) also associated LWFR formation to “large-scale advection of cold air masses into the west-central United States”.

The presence of LWFR in high-elevation *P. longaeva* trees has

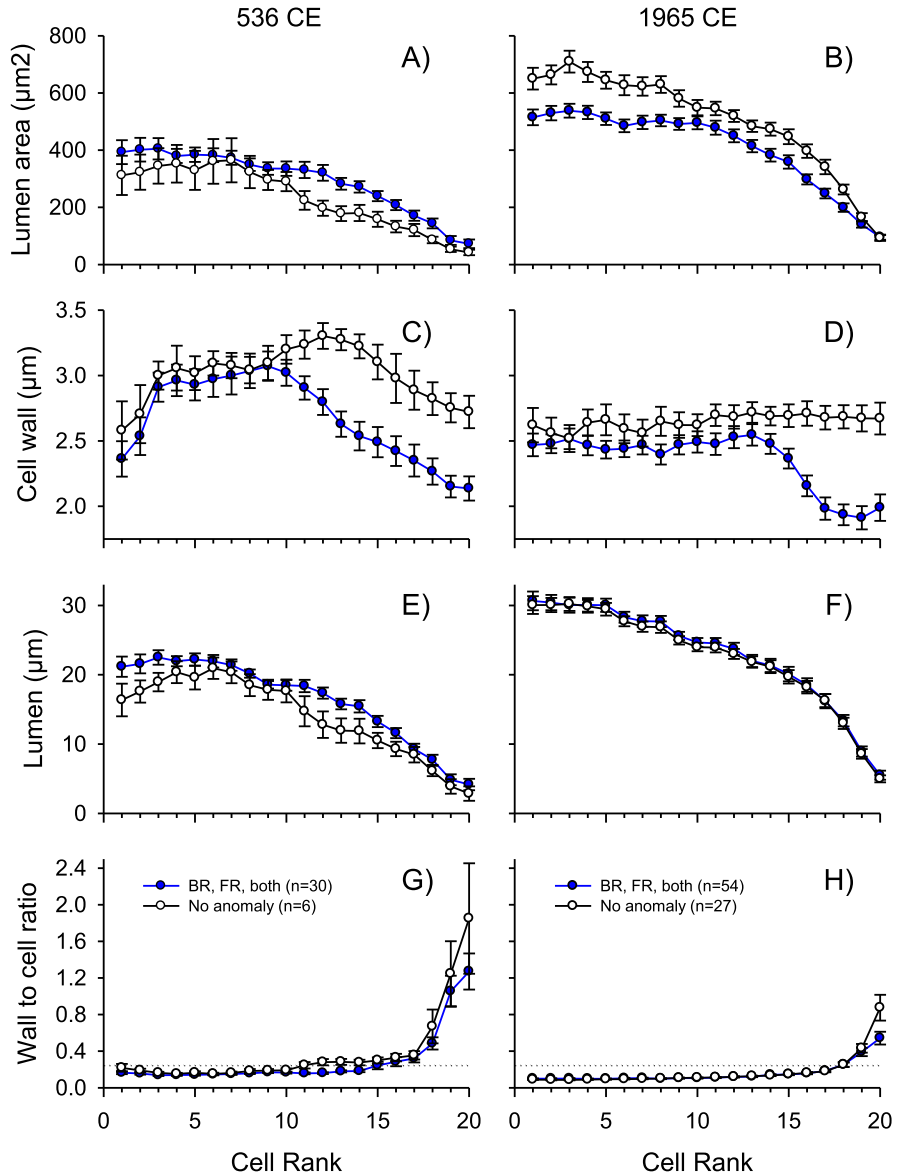


**Fig. 7.** Standardized tracheidograms for years 536 CE (left panel) and 1965 CE (right panel) and comparing tracheid features in *Pinus longaeva* trees not recording anomalies (black lines) and those recording either a blue ring, a frost ring or both (blue lines). The errors bars represent the standard error of the mean. The dotted line in G and H indicates the transition from earlywood to latewood tracheids (average cell wall/lumen ratio  $>0.25$ ). (For interpretation of the references to color in this figure legend, the reader is referred to the Web version of this article.)

been associated with volcanically-forced short-term cooling events (LaMarche and Hirschboeck, 1984; Hallman, 2001; Salzer and Hughes, 2007). In this study, years with a high frequency of BR also coincided with the years of volcanic eruptions. The well-studied “Dust Veil” period is known for three major volcanic eruptions: 536 (unsourced eruption), 540 possibly Ilopango in El Salvador (Sigl et al., 2015; Dull et al., 2019), or El Chichón in tropical Mexico, (Nooren et al., 2017), and 574 possibly Rabaul in New Britain, (Sigl et al., 2015). These eruptions lead to global low irradiance and associated climatic cooling with possible major societal impacts (Larsen et al., 2008; Sigl et al., 2015; Helama et al., 2018; Büntgen et al., 2016; Toohey et al., 2016). The 6th century eruptions are recorded in *P. longaeva* trees as narrow tree rings with numerous BR and LWFR which, again, indicates cool growing season conditions. The climate that led to the production of both BR and LWFR in 1965 has been associated with lagged cooling

conditions from the Mount Agung eruption (Indonesia) in 1963-64 (LaMarche and Hirschboeck, 1984); this was the largest and most devastating eruption of the 20th century (Self and Rampino, 2012). The 1978 tree-ring anomalies have not been associated with any known large scale volcanic activity. As far as we know, BR and LW in 1982 have not been previously linked to volcanic effects. However, the El Chichón eruption in Mexico may be related to the *P. longaeva* anomalies we found in that year. It erupted three times between March 28 and April 4, 1982 (Tilling et al., 1984). As indicated by Nooren et al. (2017), the 1982 El Chichón eruption was the most disruptive in modern Mexican history.

#### 4.4. Environmental modulation of radial growth and tree-ring anatomical variations

Our results indicated that slight changes in elevation (roughly

100 m) were sufficient to modulate the climatic conditions leading to *P. longaeva* trees recording or not a BR or a FR. Salzer et al. (2014) established that small changes in elevation (less than 100 m) near upper treeline can modulate the response of trees to climate, shifting them from being temperature sensitive to precipitation sensitive. Our BR and LWFR distributions across elevation indicate that anomalies are associated with different groups of trees depending on their position along the elevation gradient and on local topoclimate. For example, we observed that the elevation difference between trees recording and not recording a BR, a FR, or both was generally about 90–100 m. In our sample set, 6th century trees grew at a higher elevation than 20th century trees, and despite fewer samples ( $n = 12$ ), trees recording a LWFR grew at a higher elevation ( $p < 0.1$ ).

While our objective was not to assess the overall damage to trees from frost events and cool summers near the altitudinal treeline, BR and lignin deficit studies suggest that reduced lignin content in tracheids could lower embolism resistance and affect the safety of water transport and wood mechanical properties in trees (Crivellaro et al., 2018; Pereira et al., 2018). Increased porosity of the S3 layer associated with reduced lignin content could also affect the barrier between the lumen and the rest of the cell wall potentially increasing the spread of pathogens in trees (Donaldson, 1987). The direct impact of sub-freezing temperatures (and cooler growing season temperatures) at a time trees are physiologically active may affect photosynthesis inducing needle loss, death of developing shoots and mortality (Lamontagne et al., 1998). In addition to the direct physiological response, subfreezing temperature may also physically damage trees. Hiratsuka and Zalasky (1993) conducted a thorough review of potential damages associated with temperatures below freezing, alternation of freezing and melting, and accumulation of ice glaze and snow on trees. These climatically-related damages to trees may add to the complexity of the climate response in mountain environments and along short elevation gradients. For dendroclimatic studies, these elements related to elevation and topoclimate could influence the temporal stability of response to climate in trees growing fairly closed to each other and considered growing in a uniform setting.

Results from our study further support the proposition that relatively small differences in location (topographical setting) will influence the “local climate” experienced by trees which could potentially lead to mixed-climate signals in mean site chronologies. We observed that the impact of temperature may be observed at various elevations depending on the yearly climate, thus complicating the response of *P. longaeva* trees over short altitudinal gradients (100m). Our findings, in addition to those of Salzer et al. (2014), suggest that “signal dilution” in mountain environments may occur at a much finer spatial scale than previously recognized.

## 5. Conclusion

Our results provide a better understanding of how environmental conditions such as topography and climate can modulate xylem formation in *P. longaeva* trees and the resulting tree-ring anatomical features. This information can, in turn, be used to gain information about past environmental conditions in which the trees grew. Our results re-emphasize the fact that the mid-6th century and the mid-20th century were characterized by some years with cool growing seasons leading to trees recording both BR and LWFR in their annual rings. Trees growing in the mid-6th century period recorded more BR years than 20th century trees and the 6th century set of BR recorded from 539 to 542 indicates consecutive cool growing seasons. The main tracheid feature that allowed BR and LWFR to be distinguished from “normal” rings was the noticeable reduction in latewood cell wall thickness; late

growing season cellular damages from frost were only perceptible in FR. In both anomalies this reduction and lack of lignification presumably resulted from a late growing season start and a cool summer with an associated interruption of tracheid differentiation (lignification) in the late growing season due to cool temperatures affecting the rate and duration of cell wall deposition. All years that recorded LWFR also had at least one tree recording BR in that year. In years without late growing season frosts, trees recorded only BR in that year. Elevation and topoclimate were found to modulate the formation of these two anomalies. More research is needed to study the impact of reduced lignification and frost damages along short elevation gradients in regards to the temporal stability of the climate proxy provided by tree rings. Further, our results suggested that BR (microscopic) and LR (macroscopic) anomalies may originate from the same climate conditions which cause reduced lignification of the latewood tracheids. The vocabulary used to describe tree-ring anomalies at the macroscopic and microscopic scales may need to be re-examined and standardized to avoid confusion. Lastly, macroscopic distinction between thin latewood rings and LR in tree species producing narrow latewood like *P. longaeva* is challenging and may render microscopic investigation of BR inevitable in climate proxy studies especially in absence of FR.

## Data availability

The datasets generated for this study are available on request to the corresponding author.

## Author contributions

Tardif J. C.: Conceptualization, Methodology, Resources; Formal analysis, Resources, Writing - original draft preparation, Writing-Reviewing and Editing, Project administration. Salzer M.W.: Conceptualization, Methodology, Investigation, Resources, Writing - review & editing, Supervision, Project administration, and Funding acquisition. Conciori F.: Methodology, Investigation, Writing - review & editing, Visualization. Bunn A.G.: Formal analysis, Writing- Reviewing and Editing, Visualization. Hughes, M.K.: Conceptualization; Resources; Writing – reviewing and editing.

## Declaration of competing interest

The authors declare that they have no known competing financial interests or personal relationships that could have appeared to influence the work reported in this paper.

## Acknowledgement

This research was undertaken, in part, thanks to funding from the Natural Sciences and Engineering Research Council of Canada (Discovery grant to J.T.), The National Science Foundation's P2C2 program (1902625 and 1203749 to M.S and A.B with MKH co-PI on 1203749), and the Malcolm H. Wiener Foundation (M.S. collaborator). We thank Alma Piermattei, Charlotte L. Pearson, Liliana Siekacz, James A. Parks, Rex Adams, Tyler J. Tran, Stuart B. Weiss, and Jimmy Quenelle for their valuable contributions. The University of Winnipeg and The University of Arizona also supported this research. Support for the Twentieth Century Reanalysis Project version 3 dataset is provided by the U.S. Department of Energy, Office of Science Biological and Environmental Research (BER), by the National Oceanic and Atmospheric Administration Climate Program Office, and by the NOAA Physical Sciences Laboratory. We are also grateful to the reviewers and the associate editor for providing thoughtful suggestions that improved the quality of the manuscript.

## Appendix A. Supplementary data

Supplementary data to this article can be found online at <https://doi.org/10.1016/j.quascirev.2020.106516>.

## References

Baas, P., Schmid, R., van Heuven, B.J., 1986. Wood anatomy of *Pinus longaeva* (Bristlecone Pine) and the sustained length-on-age increase of its tracheids. *IAWA J.* 7 (3), 221–228. <https://doi.org/10.1163/22941932-90000988>.

Barbosa, A.C., Stahle, D.W., Burnette, D.J., Torbenson, M.C.A., Cook, E.R., Bunkers, M.J., Garfin, G., Villalba, R., 2019. Meteorological factors associated with frost rings in Rocky Mountain Bristlecone at Mt. Goliath, Colorado. *Tree-Ring Res.* 75 (2), 101–115. <https://doi.org/10.3959/1536-1098-75.2.101>.

Bräuning, A., De Ridder, M., Zafirov, N., García-González, I., Dimitrov, D.P., Gärtner, H., 2016. Tree-ring features – indicators of extreme events impacts. *IAWA J.* 2, 206–231. <https://doi.org/10.1163/22941932-20160131>.

Bruening, J.M., 2016. Fine-scale topoclimate modeling and climatic treeline prediction of Great Basin bristlecone pine (*Pinus longaeva*) in the American southwest. In: Master's Thesis Environmental Science. Western Washington University, Bellingham, WA.

Bruening, J.M., Tran, T.J., Bunn, A.G., Weiss, S.B., Salzer, M.W., 2017. Fine-scale modeling of bristlecone pine treeline position in the Great Basin, USA. *Environ. Res. Lett.* 12 (1), 14008. <https://doi.org/10.1088/1748-9326/aa5432>.

Bruening, J.M., Bunn, A.G., Salzer, M.W., 2018. A climate–driven tree line position model in the White Mountains of California over the past six millennia. *J. Biogeogr.* 45 (5), 1067–1076.

Brunstein, F.C., 1995. Bristlecone pine frost-ring and light-ring chronologies, from 569 BC to AD 1993, Colorado. In: U.S. Geological Survey, Open-File Report 95-63. US Geological Survey, p. 25.

Brunstein, F.C., 1996. Climatic significance of the bristlecone pine latewood frost-ring record at Almagre Mountain, Colorado, USA. *Arct. Alp. Res.* 28, 65–76.

Bunn, A.G., Hughes, M.K., Salzer, M.W., 2011. Topographically modified tree-ring chronologies as a potential means to improve paleoclimate inference. *Climatic Change* 8, 627–634. <https://doi.org/10.1007/s10584-010-0005-5>.

Bunn, A.G., Salzer, M.W., Anchukaitis, K.J., Bruening, J.M., Hughes, M.K., 2018. Spatiotemporal variability in the climate growth response of high elevation bristlecone pine in the White Mountains of California. *Geophys. Res. Lett.* 45, 13312–13321. <https://doi.org/10.1029/2018GL080981>.

Büntgen, U., Myglan, V.S., Ljungqvist, F.C., McCormick, M., Cosmo, N.D., Sigl, M., Jungclaus, J., Wagner, S., Krusic, P.J., Esper, J., Kaplan, J.O., de Vaan, M.A.C., Luterbacher, J., Wacker, L., Tegel, W., Kirdyanov, A.V., 2016. Cooling and societal change during the late antique little ice age from 536 to around 660 AD. *Nat. Geosci.* 9, 231–236. <https://doi.org/10.1038/ngeo2652>.

Churakova (Sidorova), O.V., Bryukhanova, M.V., Saurer, M., Boettger, T., Naurzbaev, M.M., Myglan, V.S., Vaganov, E.A., Hughes, M.K., Siegwolf, R.T.W., 2014. A cluster of stratospheric volcanic eruptions in the AD 530s recorded in Siberian tree rings. *Global Planet. Change* 122, 140–150. <https://doi.org/10.1016/j.gloplacha.2014.08.015>.

Crivellaro, A., Reverenna, M., Ruffinatto, F., Urbinati, C., Piermattei, A., 2018. The anatomy of “blue ring” in the wood of *Pinus nigra*. *Les/Wood* 67 (2), 21–28. <https://doi.org/10.26614/les-wood.2018.v67n02a02>.

D'Arrigo, R., Frank, D., Jacoby, G., Pederson, N., 2001. Spatial response to major volcanic events in or about AD 536, 934 and 1258: frost rings and other dendrochronological evidence from Mongolia and northern Siberia. *Climatic Change* 49, 239–246.

Daly, C., Halbleib, M., Smith, J.I., Gibson, W.P., Doggett, M.K., Taylor, G.H., Curtis, J., Pasteris, P.O., 2008. Physiographically sensitive mapping of climatological temperature and precipitation across the conterminous United States. *Int. J. Climatol.* 28 (15), 2031–2064. <https://doi.org/10.1002/joc.1688>.

De Micco, V., Campelo, F., De Luis, M., Bräuning, A., Grabner, M., Battipaglia, G., Cherubini, P., 2016. Intra-annual density fluctuations in tree rings: how, when, where, and why? *IAWA J.* 37, 232–259.

DeSoto, L., de la Cruz, M., Font, P., 2011. Intra-annual pattern of tracheid size in the Mediterranean *Juniperus thurifera* indicator for seasonal water stress. *Can. J. For. Res.* 41, 1280–1294. <https://doi.org/10.1139/x11-045>.

Donaldson, L.A., 1987. S3 lignin concentration in radiata pine tracheids. *Wood Sci. Technol.* 21, 227–234.

Donaldson, L.A., 1992. Lignin distribution during latewood formation in *Pinus radiata* D. Don. *IAWA J.* 13 (4), 381–387. <https://doi.org/10.1163/22941932-90001291>.

Dull, R.A., Southon, J.R., Kutterolf, S., Anchukaitis, K.J., Freudent, A., Wahl, D.B., Sheets, P., Amaroli, P., Hernandez, W., Wiemann, M.C., Oppenheimer, C., 2019. Radiocarbon and geologic evidence reveal Ilopango volcano as source of the colossal ‘mystery’ eruption of 539/40 CE. *Quat. Sci. Rev.* 222 (15), 105855. <https://doi.org/10.1016/j.quascirev.2019.07.037>.

Gärtner, H., Banzer, L., Schneider, L., Schweingruber, F.H., Bast, A., 2015. Preparing microsections of entire (dry) conifer increment cores for wood anatomical time-series analyses. *Dendrochronologia* 34, 19–23.

Gindl, W., 1999. Climatic significance of light rings in Timberline spruce, *Picea abies*, Austrian Alps. *Arctic Antarct. Alpine Res.* 31 (3), 242–246. <https://doi.org/10.1080/15230430.1999.12003304>.

Gindl, W., Grabner, M., 2000. Characteristics of spruce [*Picea abies* (L.) Karst.] latewood formed under abnormally low temperatures. *Holzforschung* 54, 9–11.

Gindl, W., Grabner, M., Wimmer, R., 2000. The influence of temperature on latewood lignin content in treeline Norway spruce compared with maximum density and ring width. *Trees (Berl.)* 14, 409–414.

Girardin, M., Tardif, J.C., Epp, B., Conciatori, F., 2009. Frequency of cool summers in interior North America over the past 3 centuries. *Geophys. Res. Lett.* 36, L07705. <https://doi.org/10.1029/2009GL037242>.

Glerum, C., Farrar, J.L., 1966. Frost ring formation in the stems of some coniferous species. *Can. J. Bot.* 44, 879–886.

Grigar, J., Čufar, K., Oven, P., Schmitt, U., 2005. Differentiation of terminal latewood tracheids in silver fir trees during autumn. *Ann. Bot.* 95 (6), 959–965. <https://doi.org/10.1093/aob/mci112>.

Gurskaya, M.A., 2014. Temperature conditions of the formation of frost damages in conifer trees in the high latitudes of western Siberia. *Biol. Bull.* 41, 187–196.

Gurskaya, M.A., Shiyatov, S.G., 2006. Distribution of frost injuries in the wood of conifers. *Russ. J. Ecol.* 37 (1), 7–12. <https://doi.org/10.1134/S1067413606010024>.

Hadad, M.A., Arco Molina, J., Roig Juñent, F.A., Amoroso, M.M., Müller, G., Araneo, D., Tardif, J.C., 2019. Frost records in tree rings linked to atmospheric circulation in northern Patagonia. *Palaeogeogr. Palaeoclimatol. Palaeoecol.* 524, 201–211. <https://doi.org/10.1016/j.palaeo.2019.03.041>.

Hadad, M.A., Tardif, J.C., Conciatori, F., Waito, J., Westwood, A., 2020. Climate and atmospheric circulation related to frost-ring formation in *Picea mariana* trees from the Boreal Plains, interior North America. *Weather and Climate Extremes* 29, 100264. <https://doi.org/10.1016/j.wace.2020.100264>.

Haldon, J., 2016. Cooling and societal change. *Nat. Geosci.* 9, 191–192. <https://doi.org/10.1038/ngeo2659>.

Hallman, C.L., 2001. Spatial Relationships in Frost Damaged High Elevation Pines and Links to Major Volcanic Eruptions. MSc. Thesis. The University of Arizona.

Hantemirov, R.M., Gorlanova, L.A., Shiyatov, S.G., 2004. Extreme temperature events in summer in northwest Siberia since AD 742 inferred from tree rings. *Palaeogeogr. Palaeoclimatol. Palaeoecol.* 209, 155–164.

Helama, S., Jones, P.D., Briffa, K.R., 2017. Dark Ages Cold Period: A literature review and directions for future research. *Holocene* 27 (10), 1600–1606.

Helama, S., Arppe, L., Uusitalo, J., Holopainen, J., Makela, H.M., Mäkinen, H., Mielikäinen, K., Nöjd, P., Sutinen, R., Taavitsainen, J.P., Timonen, M., Oinonen, M., 2018. Volcanic dust veils from sixth century tree-ring isotopes linked to reduced irradiance, primary production and human health. *Nat. Sci. Rep.* 8, 1339. <https://doi.org/10.1038/s41598-018-19760-w>.

Helama, S., Sarapää, P., Pearson, C.L., Arppe, L., Holopainen, J., Mäkinen, H., Mielikäinen, K., Nöjd, P., Sutinen, R., Taavitsainen, J.-P., Timonen, M., Uusitalo, J., Oinonen, M., 2019. Frost rings in 1627 BC and AD 536 in subfossil pinewood from Finnish Lapland. *Quat. Sci. Rev.* 204, 208–215.

Hiratsuka, Y., Zalasky, H., 1993. Frost and Other Climate-Related Damage of Forest Trees in the Prairie Provinces. Forestry Canada, Northwest Region, Northern Forestry Centre, Edmonton, Alberta. Information Report NOR-X-331.

Hirschboeck, K.K., Ni, F., Wood, M.L., Woodhouse, C.A., Dean, J.S., Meko, D.M., D.M., Swetnam, T.W., 1996. Synoptic dendroclimatology: Overview and prospectus. In: *Tree Rings, Environment, and Humanity*. Radiocarbon, Tucson, AZ, pp. 205–223.

Hoffer, M., Tardif, J.C., 2009. False rings in jack pine and black spruce trees from eastern Manitoba as indicators of dry summers. *Can. J. For. Res.* 39, 1722–1736. <https://doi.org/10.1139/X09-088>.

Hughes, M.K., Piermattei, A., Salzer, M.W., Gärtner, H., 2016. Blue Rings in Multi-Century Bristlecone Pine from Near Upper Tree Limit in California and Nevada, USA. AmeriDendro 2016, Third American Dendrochronology Conference, March 28 – April 1, 2016, Mendoza, Argentina.

Körner, C., 2012. Alpine Treelines: Functional Ecology of the Global High Elevation Tree Limits. Springer Science & Business Media, Berlin. <https://doi.org/10.1007/978-3-0348-0396-0>.

LaMarche, V.C., 1970. Frost-damage rings in subalpine conifers and their application to tree-ring dating problems. In: Smith, J.H.G., Worral, J. (Eds.), *Tree-ring Analysis with Special Reference to Northwest America*. Fac. Forest Bull. 7: 99–100. University of British Columbia, Vancouver.

LaMarche Jr., V.C., Hirschboeck, K.K., 1984. Frost rings in trees as records of major volcanic eruption. *Nature* 307, 121–126.

Lamontagne, M., Margolis, H., Bigras, F., 1998. Photosynthesis of black spruce, jack pine, and trembling aspen after artificially induced frost during the growing season. *Can. J. For. Res.* 28, 1–12.

Larsen, L.B., Vinther, B.M., Briffa, K.R., Melvin, T.M., Clausen, H.B., Jones, P.D., Siggaard-Andersen, M.-L., Hammer, C.U., Eronen, M., Grudd, H., Gunnarson, B.E., Hantemirov, R.M., Naurzbaev, M.M., Nicolussi, K., 2008. New ice core evidence for a volcanic cause of the A.D. 536 dust veil. *Geophys. Res. Lett.* 35, L04708. <https://doi.org/10.1029/2007GL032450>.

Matisons, R., Gärtner, H., Elferts, D., Kärklija, A., Adamovića, A., Jansonsa, A., 2019. Occurrence of ‘blue’ and ‘frost’ rings reveal frost sensitivity of eastern Baltic provenances of Scots pine. *For. Ecol. Manag.* 457, 117729. <https://doi.org/10.1016/j.foreco.2019.117729>.

Montwé, D., Isaac-Renton, M., Hamann, A., Spiecker, H., 2018. Cold adaptation recorded in tree rings highlights risks associated with climate change and assisted migration. *Nat. Commun.* 9 (1), 1574. <https://doi.org/10.1038/s41467-018-04039-5>.

Moreland, J., 2018. AD536 – Back to nature? *Acta Archaeol.* 89 (1), 91–111. <https://doi.org/10.1111/j.1600-0390.2018.12194.x>.

Newfield, T.P., 2018. The climate downturn of 536–550. In: Pfister, C., Mauelshagen, F. (Eds.), *The Palgrave Handbook of Climate History*. White S.

Palgrave, London, pp. 447–493. [https://doi.org/10.1057/978-1-137-43020-5\\_32](https://doi.org/10.1057/978-1-137-43020-5_32).

Nooren, K., Hoek, W.Z., Van der Plicht, H., Sigl, M., Van Bergen, M.J., Galop, D., Torrescano-Valle, N., Islebe, G., Huizinga, A., Winkels, T., Middelkoop, H., 2017. Explosive eruption of El Chichón volcano (Mexico) disrupted 6th century Maya civilization and contributed to global cooling. *Geology* 45 (2), 175–178. <https://doi.org/10.1130/G38739.1>.

Novak, K., De Luis, M., Grícar, J., Prislan, P., Merela, M., Smith, K.T., Čufar, K., 2016. Missing and dark rings associated with drought in *Pinus halepensis*. *IAWA J.* 37, 260–274.

Park, Y.-I., Dallaire, G., Morin, H., 2006. A method for multiple intra-ring demarcation of coniferous trees. *Ann. For. Sci.* 63 (1), 9–14.

Pereira, L., Domingues-Junio, A.P., Jansen, S., Choat, B., Mazzafera, P., 2018. Is embolism resistance in plant xylem associated with quantity and characteristics of lignin? *Trees (Berl.)* 32, 349–358. <https://doi.org/10.1007/s00468-017-1574-y>.

Piermattei, A., Crivellaro, A., Carrer, M., Urbinati, C., 2015. The “blue ring”: anatomy and formation hypothesis of a new tree-ring anomaly in conifers. *Trees (Berl.)* 29 (2), 613–620. <https://doi.org/10.1007/s00468-014-1107-x>.

R Core Team, 2013. R: A Language and Environment for Statistical Computing. R Foundation for Statistical Computing, Vienna, Austria. URL <http://www.R-project.org/>.

Salzer, M.W., Hughes, M.K., 2007. Bristlecone pine trees and volcanic eruptions over the last 5000 yr. *Quat. Res.* 67, 57–68.

Salzer, M.W., Hughes, M.K., Bunn, A.G., Kipfmüller, K.F., 2009. Recent unprecedented tree-ring growth in bristlecone pine at the highest elevations and possible causes. *Proc. Natl. Acad. Sci. U.S.A.* 106 (48), 20348–20353. <https://doi.org/10.1073/pnas.0903029106>.

Salzer, M.W., Bunn, A.G., Graham, N.E., Hughes, M.K., 2013. Five millennia of paleotemperature from tree-rings in the Great Basin, USA. *Clim. Dynam.* 42, 1517–1526. <https://doi.org/10.1007/s00382-013-1911-9>.

Salzer, M.W., Larson, E.R., Bunn, A.G., Hughes, M.K., 2014. Changing climate response in near-treeline bristlecone pine with elevation and aspect. *Environ. Res. Lett.* 9, 114007.

Schneider, L., Gärtner, H., 2013. The advantage of using a starch based non-Newtonian fluid to prepare micro sections. *Dendrochronologia* 31, 175–178.

Schweingruber, F.H., 2007. *Wood Structure and Environment*. Springer Science & Business Media, Heidelberg, p. 279.

Self, S., Rampino, M.R., 2012. The 1963–1964 eruption of Agung volcano (Bali, Indonesia). *Bull. Volcanol.* 74, 1521–1536. <https://doi.org/10.1007/s00445-012-0615-z>.

Semeniuc, A.I., Sidor, C.G., Popa, I., 2016. Scots pine tree ring structure modifications and relation with climate. *Eur. J. For. Sci.* 4 (2), 1–7.

Sigl, M., Winstrup, M., McConnell, J.R., Welten, K.C., Plunkett, G., Ludlow, F., Büntgen, U., Caffee, M., Chellman, N., Dahl-Jensen, D., Fischer, H., Kipfstuhl, S., Kostick, C., Maselli, O.J., Mekhaldi, F., Mulvaney, R., Muscheler, R., Pasteris, D.R., Pilcher, J.R., Salzer, M., Schüpbach, S., Steffensen, J.P., Vinther, B.M., Woodruff, T.E., 2015. Timing and global climate forcing of volcanic eruptions during the past 2500 years. *Nature* 523, 543–549. <https://doi.org/10.1038/nature14565>.

Slivinski, L.C., Compo, G.P., Whitaker, J.S., Sardeshmukh, P.D., Giese, B.S., McColl, C., et al., 2019. Towards a more reliable historical re-analysis: Improvements for version 3 of the twentieth century re-analysis system. *Q. J. R. Meteorol. Soc.* 145 (724), 2876–2908. <https://doi.org/10.1002/qj.3598>.

Stahle, D.W., 1990. *The Tree-Ring Record of False Spring in the Southcentral USA*. Ph.D. thesis, Arizona State University, Tempe, Arizona, p. 272.

Szeicz, J.M., 1996. White spruce light rings in northwestern Canada. *Arct. Alp. Res.* 28, 184–189.

Tardif, J.C., Conciatori, F., 2015. Microscopic Examination of Wood: Sample Preparation and Techniques for Light Microscopy. In: Yeung, E.C.T., Stasolla, C., Sumner, M.J., Huang, B.Q. (Eds.), *Plant Microtechniques and Protocols*. Publisher: Springer International Publishing, pp. 373–416. <https://doi.org/10.1007/978-3-319-19944-3>. Chapter: 22.

Tardif, J.C., Girardin, M.P., Conciatori, F., 2011. Light rings as bioindicators of climate change in interior North America. *Global Planet. Change* 79, 134–144. <https://doi.org/10.1016/j.gloplacha.2011.09.001>.

Tilling, R.I., Rubin, M., Sigurdsson, H., Carey, S., Duffield, W.A., Rose, W.I., 1984. Holocene eruptive activity of El Chichón volcano, Chiapas, Mexico. *Science* 224, 747–749.

Toohey, M., Krüger, K., Sigl, M., Stordal, F., Svensen, H., 2016. Climatic and societal impacts of a volcanic double event at the dawn of the Middle Ages. *Climatic Change* 136 (3), 401–412.

Tran, T.J., Bruening, J.M., Bunn, A.G., Salzer, M.W., Weiss, S.B., 2017. Cluster analysis and topoclimate modeling to examine bristlecone pine tree-ring growth signals in the Great Basin, USA. *Environ. Res. Lett.* 12, 014007.

Trouet, V., van Oldenborgh, G.J., 2013. KNMI Climate Explorer: A web-based research tool for high-resolution paleoclimatology. *Tree-Ring Res.* 69 (1), 3–13.

Vaganov, E.A., 1990. The tracheidogram method in tree-ring analysis and its application. In: Cook, E.R., Kairiukstis, L.A. (Eds.), *Methods of Dendrochronology – Applications in the Environmental Sciences*. Kluwer Academic Publishers, Dordrecht, The Netherlands/Boston, USA/London, UK, pp. 63–76.

Vaganov, E.A., Hugues, M.K., Shashkin, A.V., 2006. *Growth Dynamics of Conifer Tree Rings: Images of Past and Future Environments*. Springer, New York, USA.

Waito, J., Conciatori, F., Tardif, J.C., 2013. Frost rings and white earlywood rings in *Picea mariana* trees from the boreal plains, Central Canada. *IAWA J.* 34, 71–87. <https://doi.org/10.1163/22941932-00000007>.

Wimmer, R., 2002. Wood anatomical features in tree-rings as indicators of environmental change. *Dendrochronologia* 20, 21–36.

Wimmer, R., Strumia, G., Holawe, F., 2000. Use of false rings in Austrian pine to reconstruct early growing season precipitation. *Can. J. For. Res.* 30, 1691–1697.

Ziaco, E., Biondi, F.B., Heinrich, I., 2016a. Wood cellular dendroclimatology: Testing new proxies in great basin bristlecone pine. *Front. Plant Sci.* 1 (7), 1602. <https://doi.org/10.3389/fpls.2016.01602>.

Ziaco, E., Biondi, F., Rossi, S., Deslauriers, A., 2014a. Climatic influences on wood anatomy and tree-ring features of Great Basin conifers at a new mountain observatory. *Appl. Plant Sci.* 2 (10), 1400054. <https://doi.org/10.3732/apps.1400054>.

Ziaco, E., Biondi, F., Rossi, S., Deslauriers, A., 2014b. Intra-annual wood anatomical features of high-elevation conifers in the Great Basin, USA. *Dendrochronologia* 32, 303–312. <https://doi.org/10.1016/j.dendro.2014.07.006>.

Ziaco, E., Biondi, F., Rossi, S., Deslauriers, A., 2016b. Environmental drivers of cambial phenology in Great Basin bristlecone pine. *Tree Physiol.* 36 (7), 818–831. <https://doi.org/10.1093/treephys/tpw006>.